

Protocol

Step-by-Step Dissection of the Mediastinum: A Training Protocol

Vincenzo Verzeletti ^{1,*}, Giorgio Cannone ¹, Lena Hirtler ², Alessandro Bonis ¹, Andrea Lloret Madrid ¹, Maria Carlotta Marino ¹, Fares Shamshoum ¹, Luigi Lione ¹, Andrea Zuin ^{1,3}, Andrea Dell'Amore ^{1,*} and Federico Rea ¹

- ¹ Thoracic Surgery Unit, Department of Cardiac, Thoracic, Vascular Sciences and Public-Health, Padua University Hospital, 35121 Padua, Italy; giorgio.cannone@aopd.veneto.it (G.C.); alessandro.bonis@aopd.veneto.it (A.B.); andrea.lloretmadrid@aopd.veneto.it (A.L.M.); mariacarlotta.marino@aopd.veneto.it (M.C.M.); fares.shamshoum@aopd.veneto.it (F.S.); luigi.lione@aopd.veneto.it (L.L.); andrea.zuin@unipd.it (A.Z.); federico.rea@unipd.it (F.R.)
- ² Division of Anatomy, Center for Anatomy and Cell Biology, Medical University of Vienna, 1090 Vienna, Austria; lena.hirtler@meduniwien.ac.at
- ³ Thoracic Surgery Unit, Cardio-Thoracic Department, Udine University Hospital, 33100 Udine, Italy
- * Correspondence: vverzeletti@gmail.com (V.V.); andrea.dellamore@unipd.it (A.D.)

Abstract: The understanding of mediastinal anatomy represents a real challenge because of the vital structures inside it and due to its complex relationships with surrounding anatomical regions. Human anatomical specimens are always used both for the teaching of anatomy and the training of young surgeons, thus providing a deep understanding of the most complex anatomical regions and allowing less experienced surgeons to become familiar with surgical instruments and their use on actual human tissues. Despite the spread of these learning practices, there are no principles of dissection to follow for a young physician interested in the anatomy of the mediastinum. Therefore, the main objective of this study is to define a reliable and reproducible protocol for the dissection of the mediastinum. A stratigraphic anatomical dissection on three embalmed human specimens was performed. All steps were documented by high-quality photographs, taken with a professional digital reflex camera, and subsequently edited. A step-by-step anatomical dissection guide was created, detailing every phase, guiding the dissection of the mediastinal anatomy, and leading to the correct identification of its main anatomical structures. We present a step-by-step dissection guide to the mediastinal anatomy with point-by-point explanations and dedicated images, providing an additional tool for the comprehension of this complex anatomical area.

Keywords: anatomy of the mediastinum; dissection; surgical training; teaching



Citation: Verzeletti, V.; Cannone, G.; Hirtler, L.; Bonis, A.; Lloret Madrid, A.; Marino, M.C.; Shamshoum, F.; Lione, L.; Zuin, A.; Dell'Amore, A.; et al. Step-by-Step Dissection of the Mediastinum: A Training Protocol. *Surgeries* **2023**, *4*, 471–482. <https://doi.org/10.3390/surgeries4030046>

Academic Editor: Cornelis F. M. Sier

Received: 10 August 2023

Revised: 31 August 2023

Accepted: 8 September 2023

Published: 13 September 2023



Copyright: © 2023 by the authors. Licensee MDPI, Basel, Switzerland. This article is an open access article distributed under the terms and conditions of the Creative Commons Attribution (CC BY) license (<https://creativecommons.org/licenses/by/4.0/>).

1. Introduction

The mediastinum is defined as the anatomical region between the two pleural cavities, bordered anteriorly by the sternum, posteriorly by the thoracic vertebrae, superiorly by the thoracic inlet, and inferiorly by the diaphragmatic dome attached at the thoracic outlet. It is divided into a superior and inferior portion by a virtual plane connecting the lower margin of the fourth thoracic vertebra, posteriorly, with the manubrium–sternal joint, anteriorly. The inferior portion is additionally subdivided into three distinct parts: anterior, middle, and posterior, substantially separated by the pericardium, which delimits the middle mediastinum anteriorly and posteriorly [1]. Within this, the majority of vital thoracic structures are contained, so a detailed knowledge of the anatomy of this region is a fundamental requirement for all of those who approach this region from an anatomical, clinical, and surgical point of view.

In recent years, many universities and teaching hospitals have been equipped with dissection laboratories, not only for learning anatomy but also for the surgical training of

young residents with different surgical backgrounds, such as general surgery, orthopedic surgery, plastic surgery, head and neck surgery, and neurosurgery [2–7]. Meanwhile, several papers have been published on this topic, emphasizing how dissection optimizes learning topographical anatomy and improves resident’s surgical confidence through a wide range of procedures [8,9]. There is no doubt that this model of active learning could also be applied to cardiothoracic surgery and especially to the mediastinal anatomy [10–12].

For this reason, the main goal of this study is to define a precise and reproducible protocol, including the main steps to guide mediastinal dissection. This step-by-step dissection guide might be useful to improve the topographical knowledge and manual skills of young surgeons during routine training dissections.

2. Materials and Equipment

Three embalmed human specimens (two female, one male—all Caucasians) were carefully dissected. All the specimens came from body donations to the Center for Anatomy and Cell Biology of the Medical University of Vienna. The donors had provided written informed consent prior to death, giving permission for their bodies to be used in medical education and research. The authors hereby confirm that every effort was made to comply with all local and international ethical guidelines and laws concerning the use of human cadaveric donors in anatomical research. The bodies were embalmed with a phenol–formaldehyde solution and stored for at least 6 months prior to dissection. All the dissection procedures were conducted with standard surgical instruments (surgical and anatomical forceps, Metzenbaum scissors, Mayo scissors, straight and curve scissors, scalpels n°10–11–15–20, Gluck costotome, Beckmann retractor), paying special attention to all the surrounding soft tissues, vessels, nerves and muscles. The photographs of all dissection steps were taken using a professional reflex digital camera with a 12.3-megapixel resolution (Nikon D300, Nikon, Tokyo, Japan) coupled with a 60 mm F/2 Macro 1:1-fixed focal length lens. All pictures were subsequently edited with Adobe Photoshop 2020® (Adobe, San Jose, CA, USA) to enhance contrast and include labeling.

3. Detailed Procedure

Step 1: skin incision, soft tissue, and extrinsic muscles dissection

The dissection begins with a ‘reverse butterfly’ skin incision (Figure 1), which allows the great exposure of the thoracic cage in both the latero-lateral and cranio-caudal directions. The incision divides the thorax into two hemi-thoraxes and follows the limits of the anterior thoracic wall: superiorly for the upper margin of the first rib, inferiorly for the lower margin of the seventh, eighth, ninth, and tenth ribs, and laterally for the projection of the costal angle of the rib from the first to the tenth (Figure 1). To these incisions, another one is then conducted in the median sagittal plane, extending vertically from the upper portion of the manubrium of the sternum to the lower limit of the sternal body (Figure 1). Just at the level of the intersection between this vertical line and the cranial horizontal line, the elevation of the flap containing skin and subcutaneous tissue begins (Figure 1), which should proceed in a cranio-caudal and medio-lateral direction (Figure 1). When the hemi clavicular line is reached, it is advisable to proceed forth with a new dissection front, starting, this time, from the intersection between the vertical line and the lowest horizontal line, proceeding in a caudo-cranial and medio-lateral direction (Figure 1). In the female, the breast, localized in a superficial fascia split, is included in the skin and the subcutaneous flap.

When this maneuver is concluded, the pectoralis major muscle is exposed, which covers the pectoralis minor muscle and the anterior portion of the serratus anterior muscle. All these muscles should be gently dissected from their origins and reflected toward their respective insertions (Figure 1).

Step 2: opening the thorax

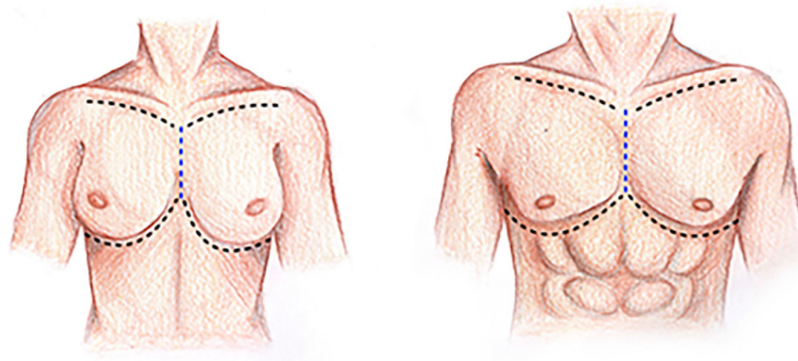


Figure 1. ‘Reverse butterfly’ skin incision. Black dotted lines: superior and inferior incision lines follow the upper margin of the 1st rib and the lower margin of the 7th, 8th and 9th. Blue dotted lines: incision line on the median sagittal plane extending vertically from the upper portion of the manubrium to the lower limit of the sternal body.

For mediastinal dissection, the thoracic cage can be opened except for its caudal lower portion. The cranial incision is identical to the one on the skin and bilaterally follows the upper margin of the first rib (Figure 2). The caudal cut extends, instead, bilaterally along the superior margin of the sixth rib into the fifth intercostal space, and it is usually clinically applied for the so-called ‘clam-shell’ thoracotomy (Figure 2). The lateral incisions join the two horizontals described above along the costal angle of the rib from the first to the sixth (Figure 2).



Figure 2. ‘Reverse butterfly’ thoracotomy. Red dotted line: superior cut along the upper margin of the 1st rib bilaterally. Green dotted line: inferior cut along the upper margin of the 6th rib bilaterally. Light blue dotted line: lateral cut along the costal angle of the rib from the 1st to the 10th. Yellow continuous line: demarcation between superior and inferior mediastinum. In the diagram, 1st: 1st intercostal space; 2: 2nd rib; 5th: 5th intercostal space; 6: 6th rib; XPS: xiphoid process of the sternum; LP: parietal peritoneum covering the liver.

It cuts along superior and inferior horizontal lines, except for extensions on the sternum, which can be made with a scalpel through the intrinsic muscles and parietal pleura, always leaning with the blade on the inferior rib of the intercostal space. A more time-consuming option may be to isolate the anterior parietal pleura from the intercostal muscles by not including it in the thoracic wall resection block; this allows the integrity of the two pleural sacs to be preserved (Figure 3).

Osteotomies on the sternum and along the lateral cuts, instead, can be performed with a hand saw, an oscillating saw, or a costotome (i.e., Gluck, Stille), being careful to not injure the underlying lungs. In order to gain space inferiorly, especially at the interface between the mediastinum and pleural cavity, it is possible to avoid the lower horizontal osteotomy in order to remove, en bloc, the whole anterior thoracic wall (Figure 2).

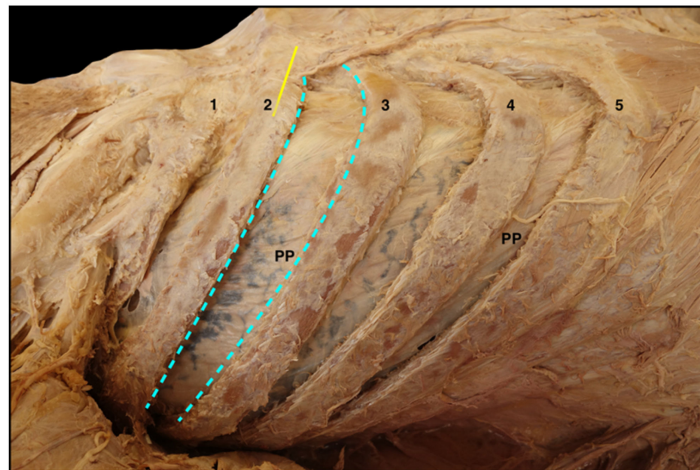


Figure 3. Dissection of the anterolateral parietal pleura from the intercostal muscles. Light blue dotted line: upper and lower limits of the anterolateral parietal pleura of the 2nd intercostal space. Yellow continuous line: demarcation between superior and inferior mediastinum. In the diagram, 1 → 5: ribs from the 1st to the 5th. PP: parietal pleura.

This gives access to the thoracic cavity, where the mediastinum and the two pleural cavities are noticeable and do not appear to be lined by the anterior parietal pleura, which is uniformly encompassed in the block of the removed thoracic wall (Figure 4); together with the pleura, internal thoracic vessels, and the transversus thoracis muscle are included in the resection block. However, they are located in its most central portion, in close relation to the inner portion of the sternum.

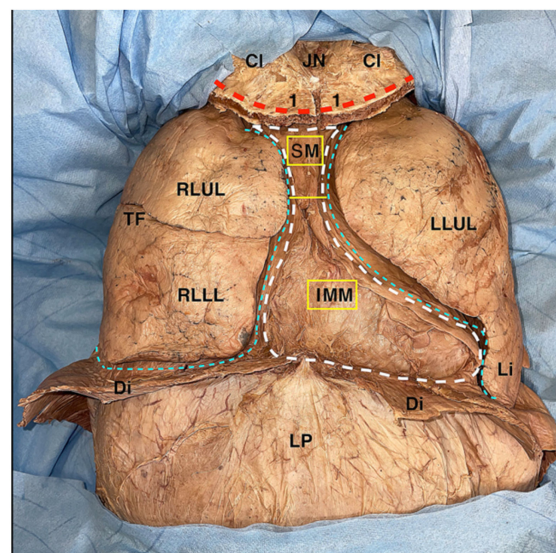


Figure 4. Thorax cavity after the removal of the thoracic wall and the anterolateral parietal pleura. Red dotted line: superior thoracotomy line. Light blue dotted lines: boundaries of the pleural cavities. White dotted line: boundaries of the mediastinum. Yellow continuous line: demarcation between superior and inferior mediastinum. JN: jugular notch; Cl: clavicular bone. 1: 1st rib; SM: superior mediastinum; IMM: inferior middle mediastinum; RLUL: upper lobe of the right lung; TF: transverse fissure; RLLL: lower lobe of the right lung; LLUL: upper lobe of the left lung; Li: Lingula of left lung; Di: diaphragm; LP: parietal peritoneum covering the liver.

Step 3: isolating the mediastinum cavity

The removal of the lungs allows an excellent visualization of the mediastinal cavity. To this purpose, the lungs are moved by hand laterally and upward to expose the hilum of

the lung and the pulmonary ligament, which are cut as close as possible to the lung. After this maneuver, the lungs are extracted from the thoracic cavity.

At this stage, the remainder of the pleural cavities may be observed and appear to be covered by the parietal pleura in all their posterior, superior, and inferior portion; the mediastinum is now exposed both anteriorly and laterally, and it is ready to be dissected (Figure 5).

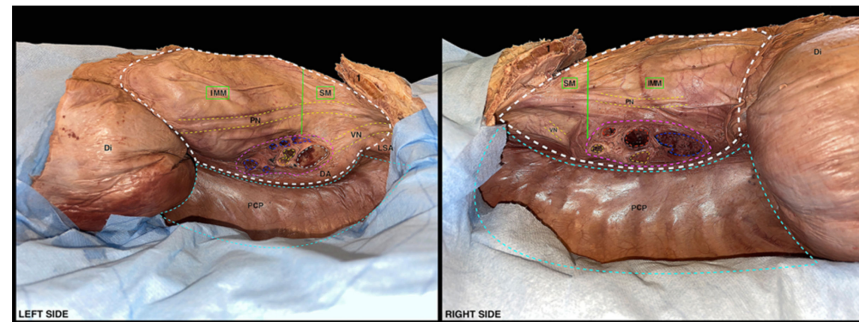


Figure 5. Lateral view of the mediastinum and of the pleural cavities after the removal of the lungs. Light blue dotted lines: boundaries of the pleural cavities. White dotted line: boundaries of the mediastinum. Green continuous line: demarcation between the superior and the inferior mediastinum. Yellow dotted lines: route of the phrenic nerve and of the vagus nerve. Pink dotted lines: boundaries of the left and hilum of the right lung. Gray dotted line: left pulmonary artery. Red dotted lines: right pulmonary arteries. Orange dotted line: left main stem bronchus at its bifurcation, right upper lobar bronchus and intermediate bronchus. Blue dotted line: left and right pulmonary veins. In the diagram, 1: 1st rib; IMM: inferior middle mediastinum; SM: superior mediastinum; PH: phrenic nerves; VN: vagus nerves; LSA: left subclavian artery; DA: descending aorta; PCP: posterior costal part of pleura; Di: diaphragm.

Step 4: dissection of the superior mediastinum

The dissection of the superior mediastinum starts with a longitudinal incision along the anterior mediastinal pleura, where the right and left pleural sacs come into contact with each other behind the upper half of the body of the sternum. The cut should be performed on the median sagittal plane in a cranio-caudal direction to the point where the mediastinal pleura continues into the superior and anterior fibrous pericardium. Once cut, the right and left mediastinal pleura can be mobilized laterally, allowing access to the structures of the superior mediastinum.

Proceeding with a delicate blunt dissection in a ventro-dorsal direction, the lower extremities of the sternohyoid, the sternothyroid muscles, and the retrosternal fat pad—the former thymus—can be appreciated. The latter can be more or less developed depending on the age of the specimen; in this case, the thymus was almost completely involuted with abundant fibro-adipose infiltration due to the donor's age.

Lateral to the adipose tissue that surrounds the retrosternal fat pad of the former thymus and just dorsal to the mediastinal pleura is the phrenic nerve, which can be adequately visualized even in the previous dissection phase (Step 3) because of its footprint on the mediastinal pleura along its entire course due to the early removal of the lungs (Figure 5). It is advisable to dissect it from the mediastinal pleura from the bottom upwards, starting from the pericardial–diaphragmatic angle (Figure 6).

By moving laterally, several structures become visible, namely the internal thoracic vein and artery and, more medially, the upper half of the superior vena cava and the two brachiocephalic veins; the right one, with its more vertical course and the left one, crossing the entire superior mediastinum to join the contralateral, form the superior vena cava (Figure 7).



Figure 6. Depiction of phrenic nerve dissection from the mediastinal pleura. Yellow dotted lines: phrenic nerve route in the mediastinum. Red dotted line: pericardiophrenic artery. Blu dotted line: pericardiophrenic vein. Black arrow: direction of dissection for phrenic nerve skeletonization. Pe: pericardium; Di: diaphragm; LP: parietal peritoneum covering the liver.

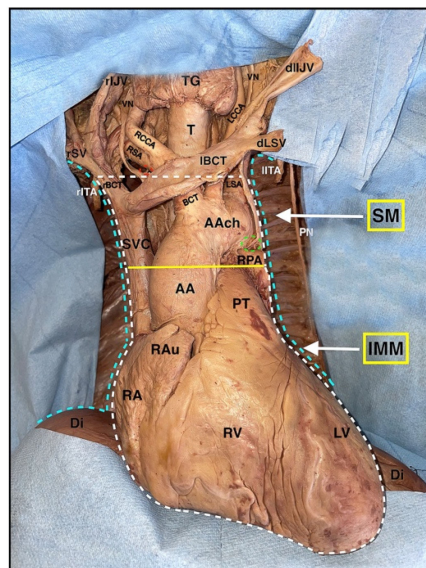


Figure 7. Superior and middle mediastinum anatomy. Light blue dotted lines: boundaries of the pleural cavities. White dotted line: boundaries of the mediastinum. Yellow continuous line: demarcation between the superior and the inferior mediastinum. Red dotted line: right recurrent laryngeal nerve. Green dotted line: left recurrent laryngeal nerve. TG: thyroid gland; rIJV: right internal jugular vein; dIJV: dissected left internal jugular vein; VN: vagus nerve; RCCA: right common carotid artery; LCCA: left common carotid artery; RSA: right subclavian artery; rSV: right subclavian vein; dLSV: detached left subclavian vein; T: trachea; IBCT: left brachiocephalic trunk; rBCT: right brachiocephalic trunk; rITA: cut right internal thoracic artery; IITA: cut left internal thoracic artery. BCT: brachiocephalic trunk; LSA: left subclavian artery; SM: superior mediastinum; IMM: inferior middle mediastinum; PN: left phrenic nerve isolated; AAch: aortic arch; SVC: superior vena cava; RPA: right pulmonary artery; AA: ascending aorta; PT: pulmonary trunk; RAu: right auricle of heart; RA: right atrium; RV: right ventricle; LV: left ventricle; Di: diaphragm.

Just caudal to the horizontal portion of the right brachiocephalic vein is where the aortic arch, the brachiocephalic trunk with the right subclavian artery, and the right common carotid artery, are located with the left common carotid artery, and the left subclavian artery (Figure 7).

Lateral to the arteries, there are the right and left vagus nerves with their left recurrent branch; the trachea, instead, is in a more dorsal position and located medially (Figure 7).

The last structures encountered are those occupying the most posterior portion of the superior mediastinum: the first tract of the thoracic part of the esophagus and the thoracic duct, which lie anterior to the thoracic vertebrae.

Step 5: dissection of the inferior mediastinum

When facing the anatomy of the inferior mediastinum, we should take into account its subdivision into an anterior, middle, and inferior portion.

○ Anterior mediastinum

The anterior mediastinum is a very narrow space between the inner facet of the body of the sternum and the pericardium. Since to remove the thoracic wall, it is necessary to dissect the main structures that engage it (connective tissue, the superior and inferior sternopericardial ligaments, lymph nodes, branches of the internal thoracic artery and vein, and the lower portion of the thymus), its dissection is normally carried out during Step 2. The anterior plane of dissection is identified between the transversus thoracic muscle and the connective tissue of the anterior mediastinum; the posterior plane is between the connective tissue of the anterior mediastinum and fibrous pericardium.

○ Middle mediastinum

Understanding the anatomy of the middle mediastinum represents a true starting point in Step 5. The dissection begins with the extension of the pre-existing incision on the median sagittal plane along the fibrous pericardium to its interface with the diaphragm and the lateral retraction of the two fibrous pericardial flaps obtained; this maneuver makes the heart immediately visible (Figure 6). Just before moving the two mediastinal pleural flaps, it is advisable to isolate the whole course of the phrenic nerve in the lower mediastinum so that it can be constantly visible even in the later stages of dissection.

For convenience, the dissection is now performed cranio-caudally, completing the skeletonization of the inferior portion of the superior vena cava and the ascending aorta; afterward, the pulmonary trunk and the ligamentum arteriosus can be isolated (Figure 7). At this point, switching laterally and observing the mediastinum through the empty pleural cavities, it is possible to appreciate the airways with the lobar bronchi, the right and left pulmonary arteries, the four pulmonary veins, and the continuation of the phrenic nerve in its route to the diaphragm (Figures 5–9). The removal of the heart and of the posterior fibrous pericardium allows the identification of the last two structures in the middle mediastinum: the arch of the azygos vein, in a right paramedian position, and more medially, the carina of trachea with two main-stem bronchi (Figure 8).

○ Posterior mediastinum

The dissection of the posterior mediastinum begins with the complete removal of the remaining mediastinal pleura, which represents its lateral boundaries.

On the right side, after the removal of the pleura, with gentle and blunt dissection, it is possible to expose the posterior intercostal arteries and veins, the intercostal nerves, and more medially, the azygos vein, which lies on the body of the thoracic vertebrae from the twelfth to the fourth (Figures 5–8). Finally, it is possible to skeletonize the right vagus nerve, which runs between the azygos vein and the right hilum of the lung, taking care to carefully preserve the largest number of its branches to the heart, lung, and esophagus (Figure 9).

On the left side, the mediastinal pleura is in contact with the adventitia of the descending aorta from the fourth to the twelfth thoracic vertebrae. Therefore, the removal of the pleura allows the identification, after blunt dissection, of the sympathetic trunk and the left vagus nerve, located inferiorly and superiorly, respectively, to the thoracic aorta. Additionally, in this case, it is advisable to preserve the branches of the left vagus nerve from which arise the parasympathetic fibers of the cardiac, pulmonary, and esophageal

plexus (Figure 9). At this point, the identification of the intercostal arteries, veins, and nerves can also be carried out on this side (Figure 9).



Figure 8. Superior, middle, and posterior mediastinum with details of the azygos veins. White dotted line: boundaries of the mediastinum after the removal of the heart. White dotted lines in the left pleural cavity: intercostal nerves from the 1st to the 8th. Yellow continuous line: demarcation between superior and inferior mediastinum. Blue dotted line: azygos vein. Light blue dotted line: hemiazygos vein. Green dotted line: accessory hemiazygos vein. TG: thyroid gland; rIJV: right internal jugular vein; dlIJV: detached left internal jugular vein; VN: vagus nerve; RCCA: right common carotid artery; RSA: right subclavian artery; rSV: right subclavian vein; dLSV: detached left subclavian vein; T: trachea; rMB: right main stem bronchus; IMB: left main stem bronchus; lBCT: left brachiocephalic trunk; rBCT: right brachiocephalic trunk; rITA: cut right internal thoracic artery; lITA: cut left internal thoracic artery. BCT: brachiocephalic trunk; LSA: left subclavian artery; SM: superior mediastinum; IMM: inferior middle mediastinum; PN: left and right phrenic nerve isolated; ST: sympathetic trunk; TE: thoracic part of the esophagus; DA: descending aorta; AArch: aortic arch; IRLN: left recurrent laryngeal nerve; SVC: superior vena cava; IVC: inferior vena cava. Di: diaphragm; 1 → 9: ribs from the 1st to the 9th.



Figure 9. An image focused on the route of the nerves in the superior and inferior mediastinum. Yellow dotted line: route of the left vagus nerve in the superior and posterior mediastinum. Light blue line: left phrenic nerve dissected in its route in the superior and in the middle mediastinum. Green dotted line: sympathetic trunk in the superior and in the posterior mediastinum. White dotted lines: intercostal nerves from the 1st to the 9th. Red dotted line: 9th intercostal artery. Blue dotted line: 9th intercostal vein. White arrows: intercostal bundles in the 7th, 8th and 9th intercostal spaces. Light blue arrow: entry of the phrenic nerve into the diaphragm. Yellow arrow: left recurrent laryngeal nerve. AA: ascending aorta; DA: descending aorta; LCCA: left common carotid artery; LSA: left subclavian artery; Di: diaphragm; 1 → 9: ribs from the 1st to the 9th.

By moving the dissection to the most central portion of the posterior mediastinum, the anterior face of the esophagus and of the descending aorta appears directly visible after the

removal of the heart and of the pericardium. Thus, after placing a self-retaining retractor (i.e., Beckamnn) between the aorta and the esophagus, it is possible to better visualize the azygos vein: the azygos vein is located in a right paramedian position and receives the hemiazygos, which proceeds from the bottom upward and the accessory hemiazygos, which proceeds from above downwards, both on the left side (Figure 8). Finally, by moving the esophagus laterally and dissecting part of the interface between its posterior wall and the thoracic vertebrae, the thoracic duct can be identified.

Focus on the mediastinal lymph nodes

Almost all the stages of mediastinal cavity dissection are characterized by the removal of abundant adipose tissue rich in lymph nodes; the dissection of such tissues should always be blunt and accurate, and there are precise spaces where these lymph nodes are organized in nine different stations (Figure 10).

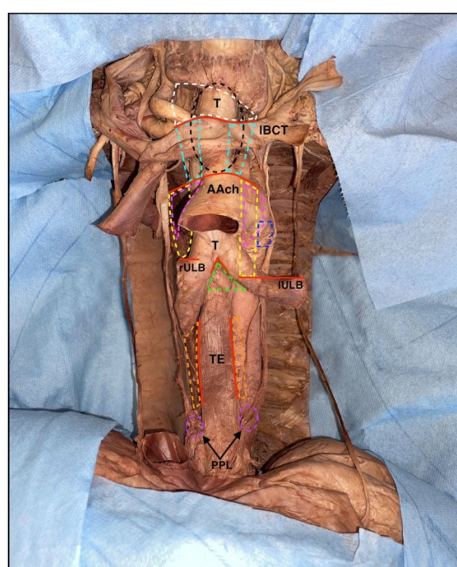


Figure 10. Image focused on mediastinal node stations. Red continuous lines: demarcation of the lymph nodes station. White dotted line: 1st station. Light blue lines: 2nd station. Black dotted line: retro-tracheal lymph nodes. Pink dotted lines: 4th station. Blue dotted line: 5th station. Yellow dotted lines: 6th station. Green dotted line: 7th station. Orange dotted lines: 8th station. Purple dotted lines: 9th station. T: trachea; LBCT: left brachiocephalic trunk; AAch: aortic arch; rULB: right upper lobar bronchus; IULB: left upper lobar bronchus; TE: thoracic part of the esophagus. PPL: parietal pleura surrounding the insertion of the pulmonary ligament.

In the first station, there are the brachiocephalic lymph nodes, which are located above a virtual line and represented by the upper margin of the horizontal tract of the left brachiocephalic vein; they are mainly paratracheal but may also be located anterior to the tracheal axis (Figure 10).

Superior paratracheal thoracic nodes are instead located between the upper margin of the horizontal tract of the left brachiocephalic vein and the upper portion of the aortic arch, and they occupy the second station (Figure 10).

With the same anterosuperior boundaries but localized posterior to the trachea, some of the superior tracheobronchial nodes are organized in the third station (Figure 10).

The inferior paratracheal thoracic nodes are placed in the fourth station, between the upper portion of the aortic arch and the superior margin of the corresponding superior lobar bronchus; in this case, the lymph nodes were located anterolaterally to the trachea, and typically they are identified during skeletonization (Figure 10).

In the fifth station, there are some of the inferior tracheobronchial nodes, localized in the aortopulmonary window, typically laterally to the ligamentum arteriosus (Figure 9). The sixth station is represented by the other inferior tracheobronchial lymph nodes, which

are placed laterally to the ascending aorta and below the upper margin of the aortic arch (Figure 10). The other inferior tracheobronchial lymph nodes are located just below the carina of the trachea and are organized in the seventh station (Figure 10). In the eighth station, there are the juxtaesophageal lymph nodes, while in the ninth, the lateral pericardial nodes are located within the pulmonary ligament (Figure 10).

4. Expected Results

As surgical procedures continue to be more challenging, the need, especially for young surgeons, for valid training in anatomy has heightened. A conscious knowledge of anatomy has, indeed, become indispensable for everyone who takes part in basic and advanced surgical training, and it is now well-established that anatomical dissection represents one of the best methods for this purpose [9].

Among the different possibilities, embalmed human bodies are known for their fidelity in the preservation of even the smallest anatomical structures, which, thanks to fixation, appear perfectly undamaged and dissectible. In addition, some of the biggest advantages of these models are their low cost and the possibility of reuse; this must be taken into account because, in different nations, body donation programs are lowering, especially during the COVID-19 era [13,14]. With regard to this, it should be emphasized that the only dissections carried out during the pandemic period were on embalmed specimens due to the capacity of formaldehyde to remove most of the pathogens [15]. This is not a minor aspect, considering that for a mediastinal dissection, it is necessary to open the thorax and the pleural cavities, with the potential risk of fluid and aerosol contact.

On the other hand, there are other anatomical models, like fresh frozen bodies, which are definitely more expensive and more difficult to manage and usually preferred for advanced surgical simulations, mainly due to their higher fidelity in tissue consistency [9].

In light of the above, the authors' idea was that the use of fixed human specimens should be considered not only for anatomical purposes but also for basic surgical training, particularly for those anatomical regions, such as the mediastinum, where the comprehension of the anatomy and the relationships between the main anatomical structures play a primary role. This concept is of particular relevance and is also emphasized by other authors, who consider fixed human specimens to be the best ones for inexpert surgeons in order to have a faithful picture of the regional anatomy [9].

The main limitation of this study is the absence, in the series of dissected cadavers, of static or dynamic systems for filling the large vessels since the mediastinal anatomy from the cadaver to a living person varies greatly for this reason [11]. However, dynamic systems, in particular, which involve the use of a pulsatile circulation model with a constant perfusion pump capable of satisfying even the basic vascular dynamics of the operating room [16,17], are very expensive and difficult to apply on a large scale. Indeed, regarding these costs, Carey et al. reported that the total cost of a single perfused specimen model was USD 1262.55: a price not affordable, especially for basic surgical training. An alternative to this is static systems, which are certainly cheaper but require specialized skills to be applied [16]. Among the latter, it is interesting to report one proposed by Dell' Amore et al. in which pulmonary vessels were injected with a colored gel after central cannulation; the presence of a viscous substance inside the vessels, such as a gel, allowed the simulation and the subsequent management of bleeding complications [12].

All of the above explains the reason why the authors decided to perform their step-by-step guide on not injected and fixed human specimens in order to reach the widest possible audience with this work.

5. Conclusions

A step-by-step dissection guide to the mediastinal anatomy, with point by point explanations and dedicated images, is presented to provide young surgeons with an additional tool in the comprehension of the mediastinal anatomy. The documented dissection was intentionally carried out by the authors on a fixed and non-injected human

anatomical specimen to make the study as accessible as possible, ranging from basic to advanced surgical training and from structures with fewer resources to richer and more experienced centers.

Author Contributions: V.V. and G.C.: Conceptualization; Data curation; Investigation; Methodology; Roles/Writing—original draft. L.H.: Conceptualization; Data curation; Investigation; Methodology; Roles/Writing—review and editing. A.B., A.L.M., M.C.M., F.S. and L.L.: Data curation; Investigation; Methodology. A.Z., A.D. and F.R.: Conceptualization; Project administration; Supervision; Validation; Visualization; Writing—review and editing. All authors have read and agreed to the published version of the manuscript.

Funding: This research received no external funding.

Institutional Review Board Statement: Not applicable.

Informed Consent Statement: The donors provided written informed consent prior to death giving permission for their body to be used in medical education and research. The authors hereby confirm that every effort was made to comply with all local and international ethical guidelines and laws concerning the use of human cadaveric donors in anatomical research.

Data Availability Statement: All data are available upon request from the corresponding author.

Acknowledgments: The authors wish to thank those who donated their bodies to science so that anatomical research could be performed. Results from such research can potentially increase mankind's overall knowledge and can then improve patient care. Therefore, these donors and their families deserve our highest gratitude.

Conflicts of Interest: The authors declare no conflict of interest.

References

1. Ugalde, P.A.; Pereira, S.T.; Araujo, C.; Irion, K.L. Correlative Anatomy for the Mediastinum. *Thorac. Surg. Clin.* **2011**, *21*, 251–272. [[CrossRef](#)] [[PubMed](#)]
2. Burns, D.M.; Bell, I.; Katchky, R.; Dwyer, T.; Toor, J.; Whyne, C.M.; Safir, O. Saturated Salt Solution Cadaver-Embalming Method Improves Orthopaedic Surgical Skills Training. *J. Bone Jt. Surg. Am.* **2018**, *100*, e104. [[CrossRef](#)] [[PubMed](#)]
3. Chai, D.Q.; Naunton-Morgan, R.; Hamdorf, J. Fresh Frozen Cadaver Workshops for General Surgical Training. *ANZ J. Surg.* **2019**, *89*, 1428–1431. [[CrossRef](#)] [[PubMed](#)]
4. Jung, H.-M.; Lee, J.-E.; Lee, S.-J.; Lee, J.-T.; Kwon, T.-Y.; Kwon, T.-G. Development of an Experimental Model for Radiation-Induced Inhibition of Cranial Bone Regeneration. *Maxillofac. Plast Reconstr. Surg.* **2018**, *40*, 34. [[CrossRef](#)] [[PubMed](#)]
5. Gualtieri, T.; Verzeletti, V.; Ferrari, M.; Perotti, P.; Morello, R.; Taboni, S.; Palumbo, G.; Ravanelli, M.; Rampinelli, V.; Mattavelli, D.; et al. A New Landmark for Lingual Artery Identification during Transoral Surgery: Anatomic-Radiologic Study. *Head Neck* **2021**, *43*, 1487–1498. [[CrossRef](#)] [[PubMed](#)]
6. Grammatica, A.; Piazza, C.; Ferrari, M.; Verzeletti, V.; Paderno, A.; Mattavelli, D.; Schreiber, A.; Lombardi, D.; Fazio, E.; Gazzini, L.; et al. Step-by-Step Cadaver Dissection and Surgical Technique for Compartmental Tongue and Floor of Mouth Resection. *Front. Oncol.* **2021**, *11*, 613945. [[CrossRef](#)] [[PubMed](#)]
7. Mattavelli, D.; Fiorentino, A.; Tengattini, F.; Colpani, A.; Agnelli, S.; Buffoli, B.; Ravanelli, M.; Ferrari, M.; Schreiber, A.; Rampinelli, V.; et al. Additive Manufacturing for Personalized Skull Base Reconstruction in Endoscopic Transclival Surgery: A Proof-of-Concept Study. *World Neurosurg.* **2021**, *155*, e439–e452. [[CrossRef](#)] [[PubMed](#)]
8. Jung, J.S.; Kang, D.H.; Lim, N.K. Face Dissection as the Plastic Surgery Approach: Effective Method in Residency Training. *J. Craniofac. Surg.* **2019**, *30*, e263–e265. [[CrossRef](#)] [[PubMed](#)]
9. Song, Y.K.; Jo, D.H. Current and Potential Use of Fresh Frozen Cadaver in Surgical Training and Anatomical Education. *Anat. Sci. Educ.* **2021**, *15*, 957–969. [[CrossRef](#)] [[PubMed](#)]
10. Robinson, D.A.; Piekut, D.T.; Hasman, L.; Knight, P.A. Cadaveric Simulation Training in Cardiothoracic Surgery: A Systematic Review. *Anat. Sci. Educ.* **2020**, *13*, 413–425. [[CrossRef](#)] [[PubMed](#)]
11. Tokairin, Y.; Nakajima, Y.; Nagai, K.; Yamaguchi, K.; Akita, K.; Kinugasa, Y. Aortic Inflation with Agar Injection Is a Useful Method of Cadaveric Preparation Which Creates a Mediastinal Anatomy That Better Mimics the Living Body for Surgical Training. *Gen. Thorac. Cardiovasc. Surg.* **2020**, *68*, 652–654. [[CrossRef](#)] [[PubMed](#)]
12. Dell'Amore, A.; Schiavon, M.; Boscolo-Berto, R.; Pangoni, A.; De Caro, R.; Rea, F. Video-Assisted Thoracic Surgery Lobectomy Simulation and Training with a New Human Cadaver Model. *Multimed. Man Cardiothorac. Surg.* **2020**, *2020*. [[CrossRef](#)]
13. Ooi, S.Z.Y.; Ooi, R. Impact of SARS-CoV-2 Virus Pandemic on the Future of Cadaveric Dissection Anatomical Teaching. *Med. Educ. Online* **2020**, *25*, 1823089. [[CrossRef](#)] [[PubMed](#)]

14. Singal, A.; Bansal, A.; Chaudhary, P. Cadaverless Anatomy: Darkness in the Times of Pandemic COVID-19. *Morphologie* **2020**, *104*, 147–150. [[CrossRef](#)] [[PubMed](#)]
15. Brassett, C.; Cosker, T.; Davies, D.C.; Dockery, P.; Gillingwater, T.H.; Lee, T.C.; Milz, S.; Parson, S.H.; Quondamatteo, F.; Wilkinson, T. COVID-19 and Anatomy: Stimulus and Initial Response. *J. Anat* **2020**, *237*, 393–403. [[CrossRef](#)] [[PubMed](#)]
16. Carey, J.N.; Minneti, M.; Leland, H.A.; Demetriades, D.; Talving, P. Perfused Fresh Cadavers: Method for Application to Surgical Simulation. *Am. J. Surg.* **2015**, *210*, 179–187. [[CrossRef](#)] [[PubMed](#)]
17. Minneti, M.; Baker, C.J.; Sullivan, M.E. The Development of a Novel Perfused Cadaver Model with Dynamic Vital Sign Regulation and Real-World Scenarios to Teach Surgical Skills and Error Management. *J. Surg. Educ.* **2018**, *75*, 820–827. [[CrossRef](#)] [[PubMed](#)]

Disclaimer/Publisher’s Note: The statements, opinions and data contained in all publications are solely those of the individual author(s) and contributor(s) and not of MDPI and/or the editor(s). MDPI and/or the editor(s) disclaim responsibility for any injury to people or property resulting from any ideas, methods, instructions or products referred to in the content.